ICSV14
Cairns • Australia
9-12 July, 2007

14th International Congress on Sound & Vibration

OPTIMAL CIRCULAR ARRAY CONFIGURATION

S.K. Lau

Department of Building Services Engineering
The Hong Kong Polytechnic University
Hung Hom, Kowloon, Hong Kong
besklau@polyu.edu.hk

Abstract

Beamforming based microphone arrays have been prove to be useful for sound source localization. It has advantage of tracking the sources in time, space and frequency domains, simultaneously. In general, the performance of beamformer will be various in terms of the beamwidth and Maximum Sidelobe Level (MSL), as a result of the configuration of the linear planar and 3-dimension arrays. Though spatial filter can adjust the beamwidth, but it is a trade off of the maximum sidelobe level. Previous works assessed the performance of microphone array with linear and specified array geometry. Multi-arm spiral and linear array location schemes have been adopted for planar array in previous studies. They are based on the combinations of circular arrays with different radii of circles and angular distances between the reference microphones of circles. Higher performance can be observed for non-redundancy array configuration, where there is no repeated vector spacing between sensors (i.e. co-array). However, the performance of the optimal multi-circular array has not yet been examined in details. The co-array pattern is indirectly controlled. The present study investigates the performance of multi-circular array. Main lobe area and the ratio of main & maximum sidelobe are investigated. Design of microphone arrays based on the optimal radii and angular distances is proposed in the present study. The results show that microphone array configuration based on the present approach has better performance on the mapping of the sound field. Design of three-circular array with seven microphone on each circle is developed.

1. INTRODUCTION

Identification of multi-moving noise sources in noise contaminated environment is critical for aeroacoustic, mechanical and environmental engineers. In past decades, beamforming based planar microphone arrays has been widely used for localization of far-field noise sources in aeroacoustic [1], automobile [2] and railway systems [3]. It has advantages of elimination of destructive interference of acoustic field in near-field measurement and provision of time-spatial-frequency analysis of noise sources. Microphone array consists of a number of microphones in a linear, planar or three-dimensional geometry. Each microphone measures the acoustical pressure as a scalar entity. The performance of the beamformer is dependent on the array pattern and the signal processing algorithms.

For configuration of planar array, the regular array (i.e. evenly distributed microphones) can results in spatial aliasing at some high frequencies. Random and quasi-random microphone array may improve the spatial aliasing [2][4], but it would make obtaining actual microphone positions difficult. Circular array with odd number of microphone spaced around the perimeter has intrinsic non-redundant co-array (vector spacing between sensors) [5]. It has been applied in the multi-arm spiral [5] and multi-arm linear [6] array location schemes, with different combinations of radii and angular distances of the reference microphones of circles. Lacoss concluded probably best spectrum window of the array can be obtained with 7 points on 3 circles of radius 16, 40 and 100 [7]. Optimal multi-circular array will be discussed at various frequencies in the present study.

2. PREFORMANCE OF CIRCULAR ARRAY CONFIGURATION

Seven microphones on each circle are investigated in present study. Figure 1 shows the configuration of two circular arrays, where R_0 and R_1 denote the radii of the circles and θ_1 the angular distance between the reference microphones of circles. The ratio of radii is $\varphi_1 = R_1/R_0$.

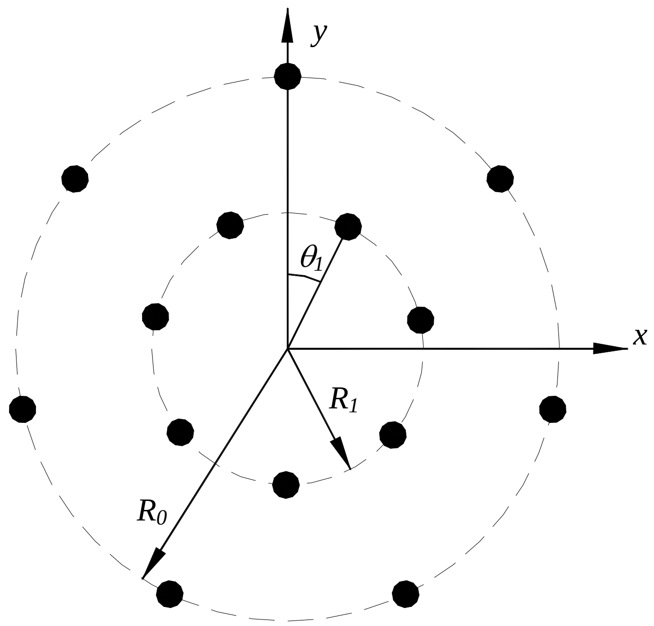

Figure 1. Configuration of two circular arrays.

The performances of the array configurations are assessed by the maximum side lobe level (MSL) and the main lobe area [2] which is the area bounded by the half-power points (3 dB) in $k_x/k \in (-1,1)$ and $k_y/k \in (-1,1)$ space. $\vec{k}$ is the wave number of the incident plane wave, while k_x and k_y are the direction components of $\vec{k}$ corresponding to the in-plane microphone coordinates x and y, respectively. The main lobe area is dimensionless in the present study. Theoretically, the optimal configuration can be found with minimum main lobe area and minimum MSL at some combinations of φ_1 and θ_1. The beam pattern of N number of microphones is the frequency-wavenumber response function evaluated versus the direction as:

$$B(\vec{k}_s, k) = \frac{1}{N}\sum_{n=0}^{N-1} a_n e^{-j(\vec{k}-\vec{k}_s)\vec{x}_n} \tag{1}$$

where $\vec{k}_s$ is the beam steering direction and $\vec{x}_n$ the in-plane coordinates from array centre (acoustic point of view) of n^{th} microphone. a_n denotes the spatial filter and are unity in the present study, and j = $\sqrt{-1}$. Without loss of generality, the beam steering direction $\vec{k}_s$ of beamformer is fixed at $k_x/k = 0$ and $k_y/k = 0$ in the present study.

2.1 Two circular arrays

For some cases, the physical dimension of the array is limited and thus the outer circle of the array is fixed to be R_0 in the present study. Radius of outer circle implies the maximum separation between the microphones and thus the maximum vectors in co-array as well as minimum main lobe area. To optimize two circular arrays, the performance of array pattern at various φ_1 between 0.1 & 1 and θ_1 between 0 & 2π/7 are investigated. Figure 2 shows the main lobe area and MSL at various combinations of φ_1 and θ_1, which are divided into 201 x 301 uniform grid points respectively throughout the computation. The frequency is represented by R_0/λ, where λ is the wavelength. The main lobe area will be enlarged as φ_1 decreases regardless θ_1, while minimum MSL can be observed at φ_1 = 0.46 regardless θ_1 at low frequency R_0/λ = 0.98 as shown in Figure 2(b). This minimum MSL regardless θ_1 shift to φ_1 = 0.18 at higher frequency of R_0/λ = 4.89 as shown in Figure 3(d). φ_1 = 1 and θ_1 = 0 (or θ = 2π/7) means the overlap of two arrays and its performance is as same as that using the configuration of single circular array with radius of R_0. Secondary circular array with radius of R_1 has not improve the main lobe area when $R_0 \geq R_1$. The trade off of MSL in expense of the main lobe area can be observed with secondary circular array.

Figure 2(a), (c) and (e) show that the percentages (rate of change) of the main lobe areas, which increases as φ_1 decreases are similar at various frequencies (between R_0/λ = 0.98 and 11.7) regardless θ_1. The main lobe area at φ_1 = 0.1 is about 2.2 to 2.5 times of that at φ_1 = 1. As frequency increases, minima of MSL observed at some combinations of φ_1 and θ_1 as shown in Figure 2(f). The improvement of beamformer from secondary circular array can be assessed by the ratios of changes of main lobe area and MSL:

$$\eta_{area} = \frac{A_0}{A_1} \quad \text{and} \quad \eta_{MSL} = 10^{(MSL_0 - MSL_1)/10}, \tag{2, 3}$$

respectively, where A_0 and A_1 is the main lobe areas of single circular array with radius of R_0 and two-circular array. MSL_0 and MSL_1 represent the maximum side lobe levels of single circular array with radius R_0 and two-circular array, respectively, in dB. The optimal two-circular array with minimum MSL at continuous and discrete frequency ranges of interest between f_1 and f_2 can be obtained by maximum points of integration and summation of the η_{MSL} over the frequency range, respectively:

$$\max(\int_{f_1}^{f_2} \eta_{MSL} df) \quad \text{and} \quad \max(\sum_{f=f_1}^{f_2} \eta_{MSL}), \tag{4, 5}$$

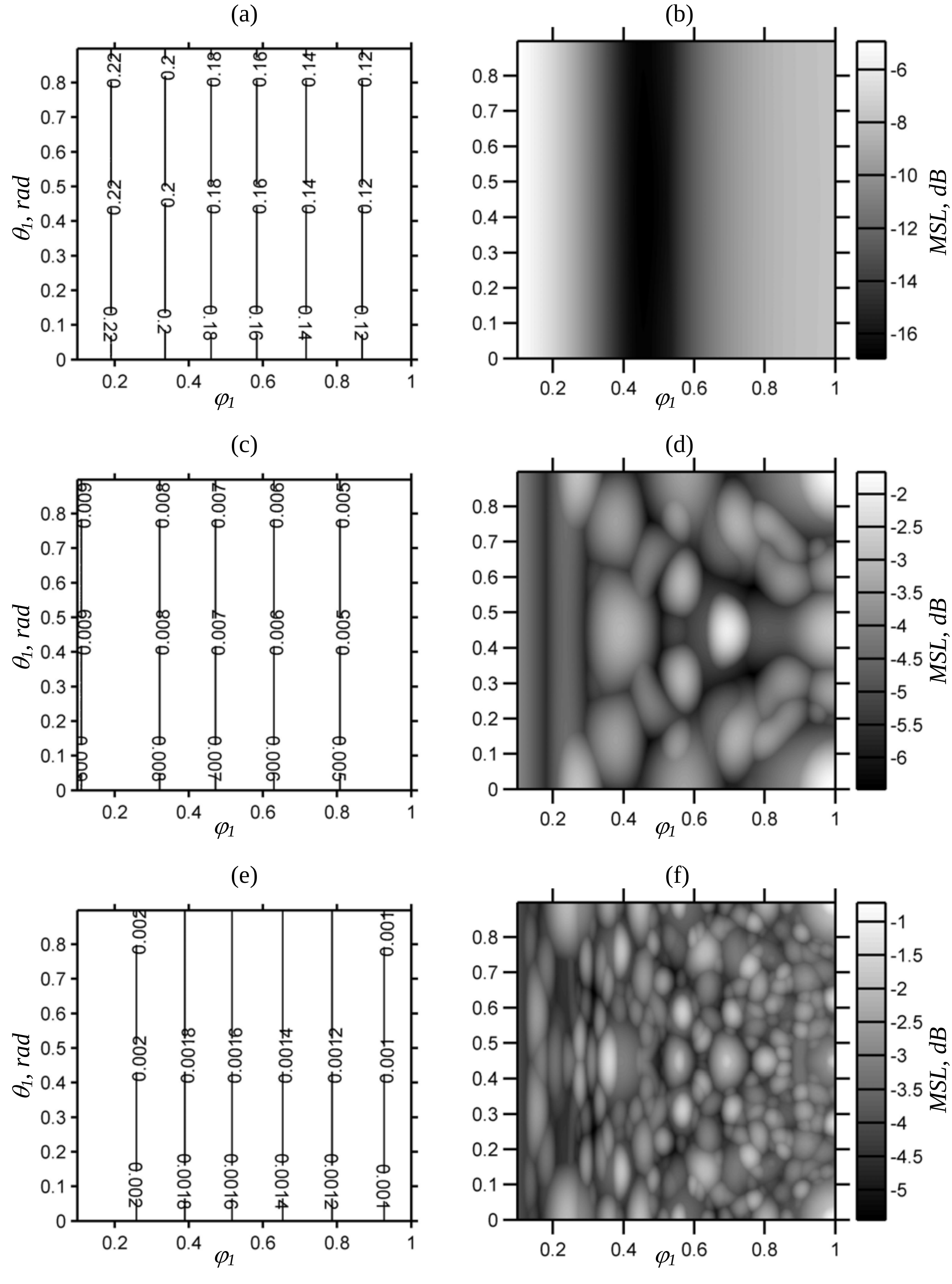

Figure 2. Variation of main lobe area and maximum side lobe level (MSL) of 2 circular array with φ_1 and θ_1. (a) and (b) at frequency R_0/λ = 0.98, respectively; (c) and (d) at frequency R_0/λ = 4.89, respectively; (e) and (f) at frequency R_0/λ = 9.79, respectively.

Figure 3(a) shows the summation of η_{MSL} over 12 uniform distributed frequencies between R_0/λ = 0.98 and 11.7. Maximum overall η_{MSL} observed with φ_1 = 0.51 and θ_1 = 0.50 rad. The η_{area} is between 0.61 and 0.55 with φ_1 = 0.51 and θ_1 = 0.50 at frequency between R_0/λ = 0.98 and 11.7. Figure 3(b) shows the summation of ($\eta_{area} \times \eta_{MSL}$) over 12 uniform distributed frequencies between R_0/λ = 0.98 and 11.7. The peak is found with φ_2 = 1 and θ_2 = 0.57 rad. Tables 1 and 2 show the η_{area} and η_{MSL} with φ_1 = 0.51 & θ_1 = 0.50 and φ_1 = 1 & θ_1 = 0.57, respectively, at various frequencies. Additional microphones on same circle of the primary circular array can eliminate the increase of main lobe area with some reduction of MSL as shown in the Figure 3(b) and Table 2. Higher reduction of MSL can be found with φ_1 < 1, especially at low frequency.

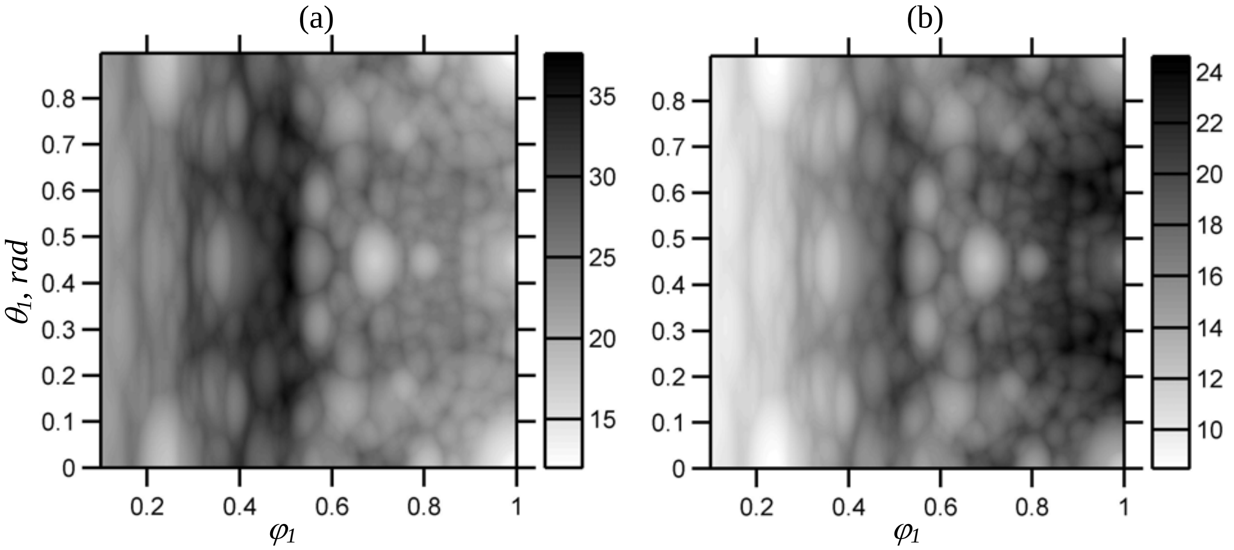

Figure 3. (a) Variation of summation of η_{MSL} for 2 circular array with φ_1 and θ_1 over 12 uniform distributed frequencies between R_0/λ = 0.98 and 11.7. (b) Variation of the summation of ($\eta_{area} \times \eta_{MSL}$) with φ_1 and θ_1 over 12 uniform distributed frequencies between R_0/λ = 0.98 and 11.7.

Table 1. η_{area} and η_{MSL} of two circular array with φ_1 = 0.51 and θ_1 = 0.50 rad at various R_0/λ.

R_0/λ	0.98	1.96	2.94	3.91	4.89	5.87	6.85	7.83	8.81	9.79	10.8	11.7
η_{area}	0.61	0.61	0.61	0.61	0.60	0.60	0.59	0.60	0.60	0.57	0.55	0.56
η_{MSL}	7.08	3.38	3.34	2.95	2.76	2.75	2.73	2.70	2.68	2.38	2.45	2.42

Table 2. η_{area} and η_{MSL} of two circular array with φ_1 = 1 and θ_1 = 0.57 rad at various R_0/λ.

R_0/λ	0.98	1.96	2.94	3.91	4.89	5.87	6.85	7.83	8.81	9.79	10.8	11.7
η_{area}	1	1	1	1	1	1	1	1	1	1	1	1
η_{MSL}	1.00	2.82	2.22	1.78	1.79	2.25	2.24	2.08	2.09	2.08	2.13	2.13

2.2 Three circular arrays

The optimal secondary circular array is set to be with φ_1 = 0.51 and θ_1 = 0.50 rad with higher improvement on MSL. The radius of the third circular array is R_2. Figure 4 shows the main lobe area and MSL at various combinations of φ_2 and θ_2, where $\varphi_2 = R_2/R_0$ and θ_2 is the angular distance between the reference microphones of circular arrays with radii of R_0 and R_2. Gradual increase of main lobe area can be again observed as φ_2 decreases regardless θ_2 as shown in Figure 4(a), (c) and (e) for $R_0 \geq R_2$. The main lobe area is increase by the third circular array if $R_0 \geq R_2$, which is a trade off of the MSL. The percentages of increase of the main lobe areas as φ_2 decreases are similar at various frequencies (between R_0/λ = 0.98 and 11.7) regardless θ_2, which is about double (1.9 to 2.1 times) of the main lobe area from φ_2 = 1 to 0.1. Minimum MSL is at φ_2 = 0.36 regardless θ_2 at low frequency R_0/λ = 0.98 as shown in Figure 4(b). This minimum MSL shift to φ_2 = 0.19 at higher frequency R_0/λ = 4.89 as shown in Figure 4 (d). As frequency increase, Figure 4(f) shows discrete minima of MSL at higher frequencies. Maximum overall η_{MSL} observed with φ_2 = 0.33 and θ_2 = 0.63 rad over 12 uniform distributed frequencies between R_0/λ = 0.98 and 11.7 as shown in Figure 5(a). The η_{area} is between 0.58 and 0.53 with φ_2 = 0.33 and θ_2 = 0.63 rad at frequency between R_0/λ = 0.98 and 11.7. Optimal configuration obtained when minimum of both main lobe area and MSL can be achieved. Figure 5(b) shows the summation of ($\eta_{area} \times \eta_{MSL}$) over 12 uniform distributed frequencies between R_0/λ = 0.98 and 11.7. The peak is found with φ_2 = 0.93 and θ_2 = 0.34 rad. Tables 3 and 4 show the η_{area} and η_{MSL} with φ_2 = 0.33 & θ_2 = 0.63 and φ_2 = 0.93 & θ_2 = 0.34, respectively, at various frequencies.

Table 3. η_{area} and η_{MSL} of three circular array with φ_2 = 0.33 and θ_2 = 0.63 rad at various R_0/λ.

R_0/λ	0.98	1.96	2.94	3.91	4.89	5.87	6.85	7.83	8.81	9.79	10.8	11.7
η_{area}	0.58	0.58	0.58	0.58	0.58	0.57	0.57	0.56	0.56	0.57	0.55	0.53
η_{MSL}	4.41	2.25	2.42	1.97	1.57	2.33	2.33	2.29	2.29	2.30	2.44	1.53

Table 4. η_{area} and η_{MSL} of three circular array with φ_2 = 0.93 and θ_2 = 0.34 rad at various R_0/λ.

R_0/λ	0.98	1.96	2.94	3.91	4.89	5.87	6.85	7.83	8.81	9.79	10.8	11.7
η_{area}	0.94	0.94	0.94	0.94	0.94	0.94	0.94	0.94	0.94	0.94	0.93	0.93
η_{MSL}	0.91	3.97	1.17	1.65	1.65	2.44	2.07	2.07	2.07	2.09	2.22	1.84

3. CONCLUSIONS

Optimal two and three circular arrays have been investigated in the present study. The additional circular array results increase of the main lobe area regardless the angular distance between the reference microphones of the circles, as its radius is smaller than the primary circular array. The main lobe area can be maintain with reduced maximum side lobe level (MSL) using the secondary and third circular arrays with radius as same as that of the primary circular array. There are minimum MSL at optimal radii of secondary and third circular arrays regardless of the angular distances between the reference microphones of the circles at low frequency. Minima of MSL occur at some combinations of radii of secondary & third circular arrays and angular distances between the reference microphones of the circles at higher frequencies. Optimal configuration can be found by integration and summation of the normalized MSL and main lobe area over the frequency range of interest. There may be two choices for the optimization of each circle. One is the minimized MSL priority with possibly smaller radius of additional circle, and another is minimized main lobe area priority with possibly larger radius of circle. With minimized MSL approach, the optimal radii ratio is R_0 : R_1 : R_2 = 1 : 0.51 : 0.33 for seven microphones on each circle. The corresponding angular distances between reference microphones are θ_1 = 0.50 rad and θ_2 = 0.63 rad for the frequencies between R_0/λ = 0.98 and 11.7.

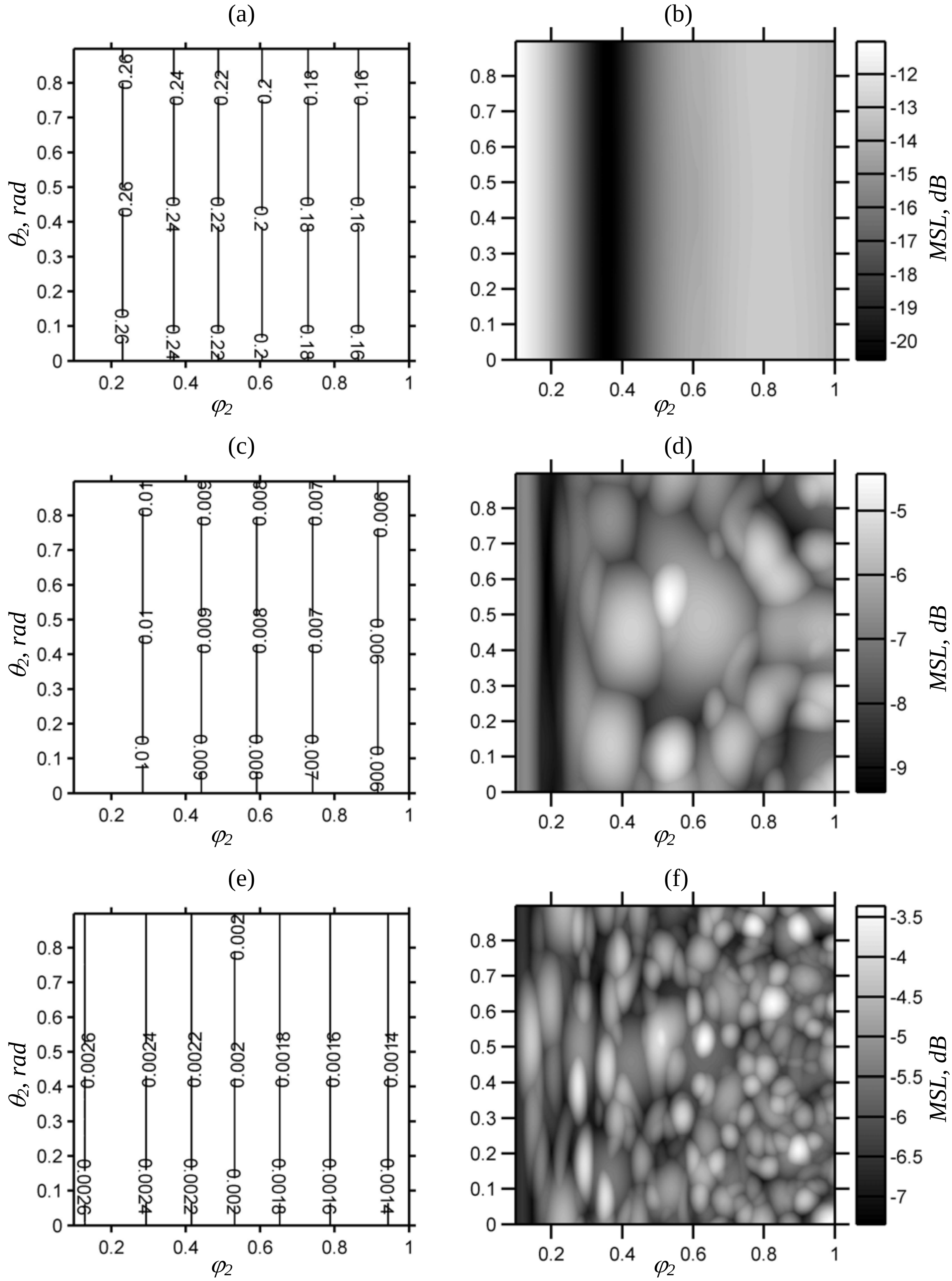

Figure 4. Variation of main lobe area and maximum side lobe level (MSL) of 3 circular arrays with φ_2 and θ_2. (a) and (b) at frequency R_0/λ = 0.98, respectively; (c) and (d) at frequency R_0/λ = 4.89, respectively; (e) and (f) at frequency R_0/λ = 9.79, respectively.

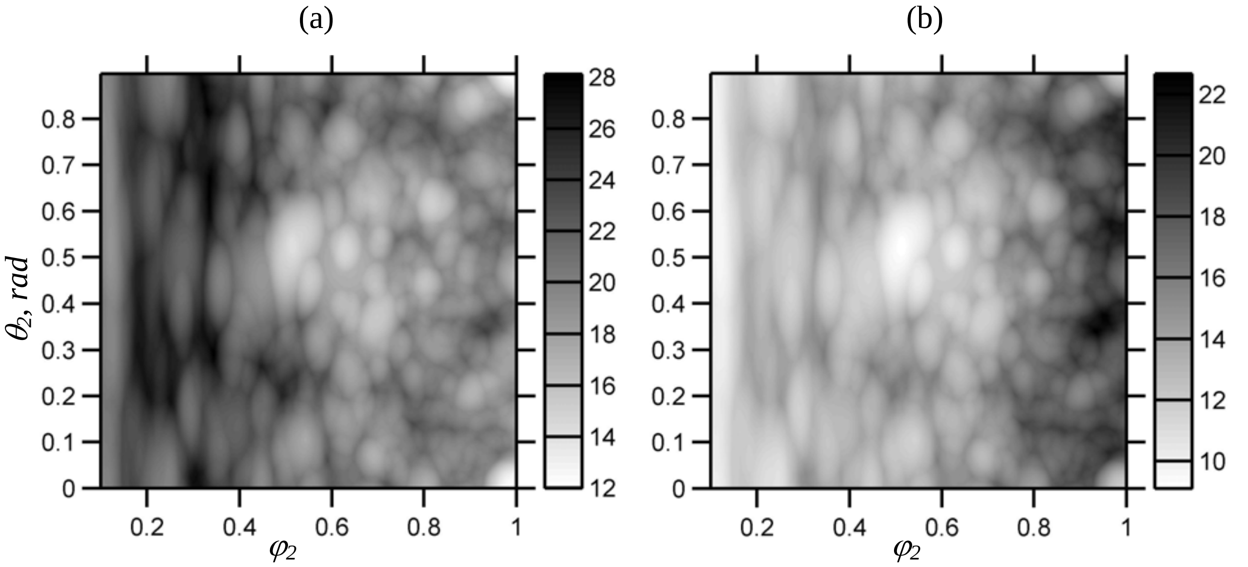

Figure 5. (a) Variation of summation of η_{MSL} for 3 circular array with φ_2 and θ_2 over 12 uniform distributed frequencies between R_0/λ = 0.98 and 11.7. (b) Variation of the summation of ($\eta_{area} \times \eta_{MSL}$) with φ_2 and θ_2 over 12 uniform distributed frequencies between R_0/λ = 0.98 and 11.7.

4. ACKNOWLEDGEMENTS

The work described in this paper was fully supported by a grant from the Hong Kong Polytechnic University (Project A/C code: G-YF22)

REFERENCES

[1] T.F. Brooks and W.M. Humphreys, "A deconvolution approach for the mapping of acoustic sources (DAMAS) determined from phased microphone arrays", *Journal of Sound and Vibration* **294**, 856-879 (2006).

[2] S. Zheng, F. Xu, X., Lian, D. Yang, Y. Luo and K. Li, "Generation method of two-dimensional random array for locating noise sources on moving vehicles", *Proceedings of Inter-NOISE 2006*, Honolulu, Hawaii, USA, 3 – 6 December 2006, on CD-ROM.

[3] B. Schulte-Werning, K. Jäger, R. Strube and L. Willenbrink, "Recent developments in noise research at Deutsche Bahn (noise assessment, noise source localization and specially monitored track)", *Journal of Sound and Vibration* **267**, 689-699 (2003).

[4] P. Wang and S. Jasti, "Design of quasi-random microphone array", *Proceedings of INTER-NOISE 2006*, Honolulu, Hawaii, USA, 3 – 6 December 2006, on CD-ROM.

[5] T.J. Mueller (Ed.), *Aeroacoustic measurements*, Springer, 2002.

[6] J.J. Christensen and J. Hald, "Beam forming array of transducers". *US Patent No. 7,098,865 B2*. (2006)

[7] R.T. Lacoss, "Geometry and patterns of large aperture seismic arrays", *Mass. Inst. Of Tech. Technical Note 1965-64*. (1965)